ELSEVIER

PII: S0032-3861(97)00275-9

Polymer Vol. 39 No. 2, pp. 387–392, 1998

0032-3861/97/$17.00+0.00

A study of the surface viscoelasticity of poly(vinyl acetate) at the air–water interface using the electrocapillary wave diffraction technique

Randy Skarlupka[a,b], Yongsok Seo[a,c,*] and Hyuk Yu[a]

[a]*Department of Chemistry, University of Wisconsin, 1101 University Avenue, Madison, WI 53706, USA*

[b]*Permanent address: Polymer Composites Incorporated, 4610 Theurer Boulevard, P.O. Box 30010, Winona, MN 55987-1010, USA*

[c]*Permanent address: Polymer Processing Laboratory, Korea Institute of Science and Technology (KIST), P.O. Box 131, Cheongryang, Seoul, Korea*

(Revised 1 April 1997)

The surface viscoelastic properties of poly(vinyl acetate) (PVAc), spread as a monolayer at the air–water interface, were determined using the electrocapillary wave diffraction (ECWD) technique with the Wilhelmy plate method for static surface tension measurements. Surface longitudinal viscosity, κ, and elasticity, ε, were calculated from the dispersion equation for surface waves over a range of surface concentrations. The static and dynamic elasticities were in agreement at the low surface concentrations but showed some differences at higher concentrations. The difference in surface viscoelastic properties measured by ECWD and by surface quasi-elastic light scattering (SLS) was ascribed to the difference in monolayer response to waves of different wavelengths. Because of the relatively long wavelengths of ECWD capillary waves, the monolayer surface elasticities measured by ECWD were smaller than the static elasticities in the concentration range where maximum damping due to the resonance between the longitudinal wave and the transverse capillary wave occurs. © 1997 Elsevier Science Ltd.

(Keywords: poly(vinyl acetate); surface viscoelasticity; electrocapillary wave diffraction)

INTRODUCTION

Thin films made from surface-active polymers spread at the air–water (A–W) interface are both scientifically and technologically interesting. Many experimental studies have been performed using several methods, including ellipsometry, capillary wave techniques, and X-ray and neutron reflectometry in conjunction with a method to determine surface pressures[1–11]. The study of monolayers of surface-active polymers spread at the A–W and oil–water (O–W) interfaces provides a basis for understanding the behaviour and conformation of molecules. These structures are of prime relevance in the investigation of the stability of emulsions and foams, since there is a strong correlation between the stability and mechanical strength of interfacial films. PVAc is one of the most heavily investigated polymers because of its surface activity and its property of spreading readily to form films stable up to high surface pressures (15 mN m^{-1})[12]. In our laboratory, PVAc monolayer film properties were studied systematically using the surface quasi-elastic light scattering (SLS) and Wilhelmy plate methods[1,12–15].

The principles of SLS and electrocapillary wave diffraction (ECWD) are the same[16]: both provide dynamic information on the liquid surface. However, they differ principally in two respects. First, the frequency range of interest is set by the scattering angle range, i.e. momentum transfer, in SLS, whereas it is set by the imposed frequency range of the external field in ECWD. Second, the wave damping in SLS is provided in the temporal domain, whereas that in ECWD is in the spatial domain, so that some differences exist in the frequency ranges detected by the two methods. As mentioned by Miyano[16], the hydrodynamic description of the surface waves does not of course depend on how the waves are generated, e.g. mechanically or thermally. Therefore the dispersion relation should be identical in both cases. Experimentally, however, there is one distinction between the two approaches. In the SLS experiment with thermally fluctuating surfaces, the time evolution of a wave of a selected wavelength is studied, i.e. the complex frequency ($\omega = \omega_r - i\omega_i$) is measured as a function of the real wavenumber ($k = k_r$). On the other hand, for ECWD experiments in which the surface waves are externally generated, their frequency is fixed and real ($\omega = \omega_r$), but a complex wavenumber ($k = k_r + ik_i$) is measured. The dispersion relation is therefore seen from a different perspective[16,17].

Besides having a different detection frequency range[18] (<5 kHz), ECWD offers an advantage over the SLS technique: whereas SLS relies on thermally induced spontaneous capillary waves at both liquid–liquid and air–liquid interfaces, ECWD takes an alternative approach, in which capillary waves of the desired frequency are externally generated through an AC electrical field. In the propagating wave regime, the SLS technique has a fairly

* To whom correspondence should be addressed.

low viscosity limit (~5 mPa s). On the other hand, the theoretical upper limit of viscosity for ECWD in the same regime is of the order of 10^2 mPa s[18]. ECWD is also regarded as non-invasive, because the ratio of amplitude to wavelength of the induced capillary waves is of the order of 10^{-4}.

This paper reports an examination of the dynamic surface viscoelastic properties of PVAc spread as a monolayer at the A–W interface, using ECWD.

EXPERIMENTAL

Materials

PVAc was polymerized by free-radical polymerization and purified by precipitation in methanol[14]. Only one fraction, with a molecular weight of 114 000, was used for this study. Earlier, it was shown[13] that there exists no molecular weight dependence for PVAc in SLS experiments in the range 55K–1150 K. In the present study, chloroform (h.p.l.c. grade, Aldrich) was used without further purification as the spreading solvent. All glassware and Teflon apparatus were cleaned with a sulfuric acid–Nochromix (Godax Labs, Inc. New York) solution. Distilled water, further purified by a Millipore Q_2 ion exchange and filtration system, was used as the subphase.

Surface pressure measurements

The surface pressure experiments were performed using a Teflon trough (285 × 110 × 12.5 mm) with a sliding barrier placed in a Plexiglass cabinet to maintain constant high humidity[13]. The temperature of the subphase was controlled by circulating water at 25.0 ± 0.1°C through a glass coil placed at the bottom of the trough. After the trough was set up, the water surface was cleaned by wiping with the moving bar and gently aspirating the surface. Before the experiments were begun, at least 30 min was allowed to reach thermal equilibrium. For the spreading solvent, it was ascertained that the addition of an amount of pure solvent comparable with that used in surface studies of PVAc causes no change in water surface tension. Surface tension was measured with a Cahn electrobalance (Model 2000) with a sandblasted platinum Wilhelmy plate(11 × 26 × 0.1 mm). The plate was stored in HNO_3–H_2SO_4 and carefully rinsed with distilled THF and Millipore water and dried before use. In this study, both the continuous addition method, using a Hamilton syringe, and the stepwise compression method were used to prepare the surface layer. Since PVAc is insoluble in water, it was assumed that the surface mass density was conserved during the measurement.

Electrocapillary wave diffraction measurements

Since the ECWD apparatus and the attendant instrument details have been described elsewhere[19], only the basic scheme of the apparatus is outlined here. Electrocapillary waves in the frequency range 0.1–4 KHz are excited by applying an intense local AC electric field over a small surface area at the air–liquid interface through a source needle positioned within ~100 μm of the interface. Others have used a razor blade instead of a needle[19], since a razor blade can generate capillary waves with larger amplitudes. However, as shown in our previous studies, use of a needle rather than a razor blade has several advantages even though the waves generated damp more rapidly than those generated by razor blade. The advantages are: (1) a possible edge effect of the blade can be avoided; (2) non-planarity in the detection of generated waves in cases in which the blade axis is not perfectly parallel with the interface can be avoided; and (3) errors likely in determinations of the displacement distance r from the source axis can be eliminated by placing the laser beam scanning axis off the perpendicular to the razor blade line. By applying an AC electric field, because of a difference in dielectric permittivity across the interface, circular ripples with a spatial wavelength in the region of 0.3–3 mm and an amplitude/wavelength ratio of the order of 10^{-3} to 10^{-5} are generated, so that the measurements are macroscopic in character, as is required in any viscoelastic measurement[20].

The spatial wavevector k_0 and the corresponding wave damping coefficient β for the capillary waves thus determined are then used in the following dispersion equation for surface waves to deduce the surface tension γ or interfacial tension σ and the bulk shear viscosity of one fluid phase η:

$$[\varepsilon^* k^{*2}/\omega + i\eta(k^* + m) + i\eta'(k^* + m')]$$

$$[i\eta(k^* + m) + i\eta'(k^* + m')$$

$$+ \sigma^* k^{*2}/\omega + g(\rho - \rho')/\omega - \omega(\rho + \rho')/k^*]$$

$$+ [\eta(k^* - m) - \eta'(k^* - m')]^2 = 0 \qquad (1)$$

where $k^* = k_0 + i\beta$, $m \equiv [k^{*2} + i\omega\rho/\eta]^{1/2}$, $m' \equiv [k^{*2} + i\omega\rho'/\eta']^{1/2}$, ω is the angular frequency, g is the gravitational acceleration, η and η' are the shear viscosities of air (or upper phase) and subphase respectively, ρ and ρ' are the corresponding densities, $\varepsilon^* \equiv \varepsilon + i\omega\kappa$, where ε is the dynamic surface dilational elasticity and κ is the corresponding viscosity, and $\sigma^* \equiv \sigma + i\omega\mu$, where σ is the dynamic surface tension and μ is the transverse viscosity. The dilational storage and loss components, ε and κ, of the complex modulus ε^* are calculated from experimentally determined values of k_0 and β at fixed ω by assuming that μ, the transverse viscosity, is zero[18,20], so that σ^* is equal to the static surface tension σ, which in turn is accessible experimentally by means of conventional static techniques such as the Wilhelmy plate method. Recently, Earnshaw and co-workers investigated experimentally by SLS a case in which the transverse viscosity was non-zero for soluble surfactants[5,21–24]. However, their results were obtained at very high wavenumbers and high frequencies, conditions that are beyond the scope of ECWD experiments. At the high frequency values, negligible transverse viscosity can be amplified because of multiplication by the frequency, i.e. $\omega\mu$. The transverse viscosity, if any, is small at the frequencies used in the externally excited waves, as verified experimentally by Earnshaw *et al.*[25]. The surface concentration at which the transverse viscosity has a non-zero value is extremely dilute[12]. This is beyond the experimental bounds of the current study. Though computer analysis of the effect of the transverse viscosity is possible, its physical meaning should be more carefully assessed. This subject merits further investigation, since it can be linked with certain relaxation processes depending on experimental conditions[12,16,19]. This issue is addressed later. The instrument was calibrated with the surface tensions of water and toluene and the interfacial tension of heptane–water, on the assumption that ε^* is zero for pure liquids[18].

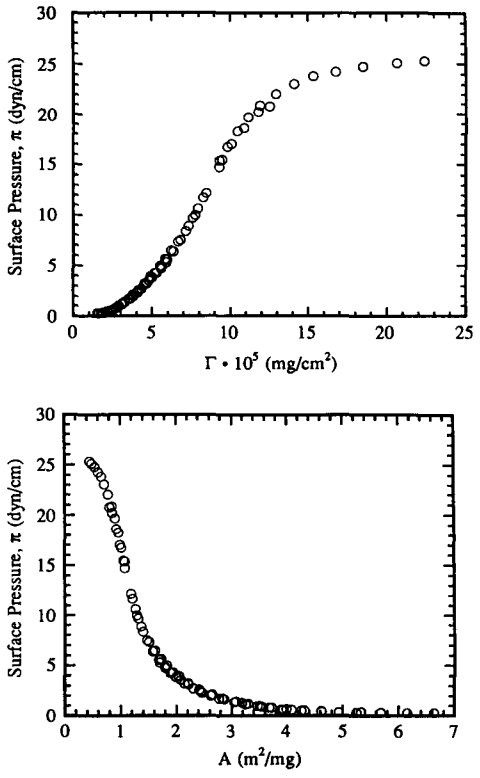

Figure 1 (a) Static surface pressure for PVAc spread at the air–water interface ($T = 25°C$), as a function of (a) surface concentration, (b) surface area per unit mass

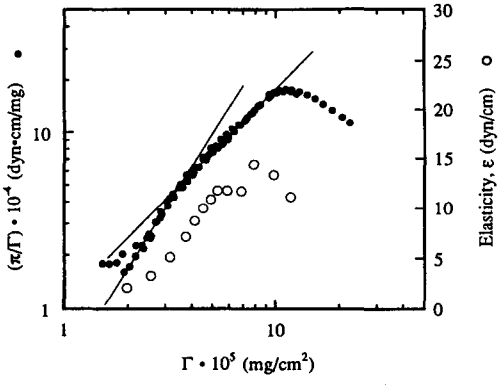

Figure 2 Double-logarithmic plot of π/Γ versus Γ for PVAc spread at the air–water interface ($T = 25°C$). The dynamic surface elasticity is also plotted as a function of surface concentration to show the relative position of the plateau with respect to the break in the slopes

RESULTS AND DISCUSSION

Figure 1a shows a plot of surface pressure π *versus* surface concentration Γ. These values were obtained using the Wilhelmy pate method. Surface concentration was varied by film compression. The most significant change in surface pressure occurred over the concentration range from 7×10^{-5} to 10×10^{-5} mg cm^{-2}, and the surface pressure appeared to level off in the vicinity of $\pi = 26$ mN m^{-1}, because the surface pressure did not show any change with decreasing surface area. The collapse pressure of 26 mN m^{-1} is in agreement with our previous results[14] and others reported in the literature[26]. In *Figure 1b*, the data in *Figure 1a* are replotted as a function of surface area per unit mass. The limiting area A_0, deduced by extrapolation to $\pi = 0$ of the straight portion of the π–A curve at high

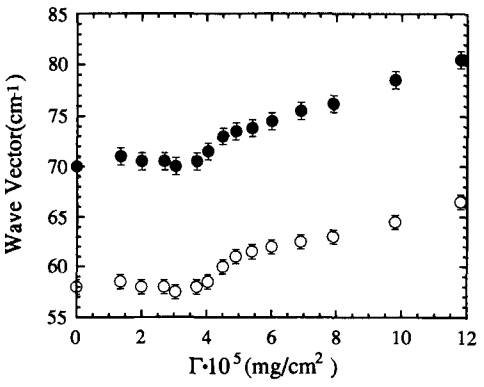

Figure 3 Wavevector as a function of surface concentration for PVAc spread at the air–water interface ($T = 25°C$). Only two of the eight frequencies examined are represented here: ○, 600 Hz; ●, 800 Hz

surface pressures, was found to be 1.75 m^{2}mg^{-1} and the increase in A_0 corresponds to the limiting surface concentration, $\Gamma = 5.71$ mg cm^{-2}. A monomer unit area of 25 Å^2 obtained from the A_0 value is also in agreement with previous results reported in the literature[14].

Figure 2 is a typical double-logarithmic plot of π/Γ versus Γ for PVAc, which clarifies the surface concentration dependence of surface pressure. Again this shows the reproducibility of our previous results on the same sample. We have already discussed five distinct regions in our previous work[14]: (1) the dilute region below 2×10^{-5} mg cm^{-2}; (2) the region between $2 \times 10^{-5}$and 4×10^{-5} mg cm^{-2}; (3) the region from 4×10^{-5} to 10×10^{-5} mg cm^{-2}, where another straight line with decreased slope can be drawn; (4) the region $10 \times 10^{-5} < \Gamma < 20 \times 10^{-5}$ mg cm^{-2} where the slope gradually changes from positive to negative; and (5) the region above $\Gamma = 20b \times 10^{-5}$ mg cm^{-2}, where the data almost fit a straight line with a negative slope. In the final region (5), the surface tension no longer depends on surface concentration. Region (2) is regarded as a semidilute region because the value of the slope, 1.8, is well established according to the scaling theory of polymers in two dimensions, amply verified experimentally in the literature[27–29].

We now turn to the ECWD results. For the ECWD experiments, the surface concentration was varied by the continuous addition method to prepare the surface layers, using a Hamilton syringe. The waiting time for each aliquot addition to allow for evaporation of the spreading solvent and reach equilibrium was 2 h. *Figures 3 and 4* show plots of wavevectors and damping constants as functions of surface concentration for two different frequencies. It seems that the variation in the damping constant with increasing surface concentration provides a sensitive indication of structural changes. As well noted in the literature[2,3,26], coverage with a monolayer gives elastic properties to a surface so that it tends to resist the periodic surface expansion and compression that accompany wave motion. For the transverse capillary waves, whose amplitudes are much smaller than the wavelength, the surface energy is dominant with respect to the hydrostatic process as a restoring force after deviation of the surfaces normal to the interface[30]. On the other hand, longitudinal waves, accompanied by horizontal rather than vertical surface movement, are forced upon most liquid layers (or surface-covering monolayers) by the non-zero tangential surface stress, which gives rise to more vorticity and hence to higher energy dissipation[30–32]. The existence of longitudinal

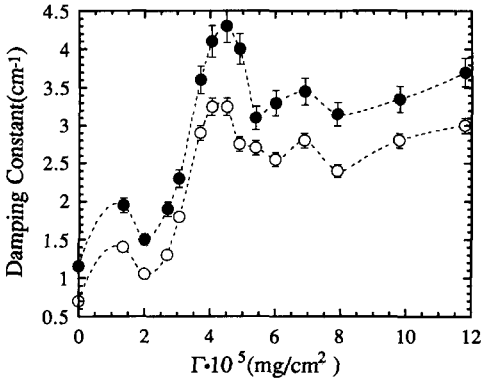

Figure 4 Damping constant as a function of surface concentration for PVAc spread at the air–water interface ($T = 25$°C): ○, 600 Hz; ●, 800 Hz. The dashed lines are meant as a guide for the eye

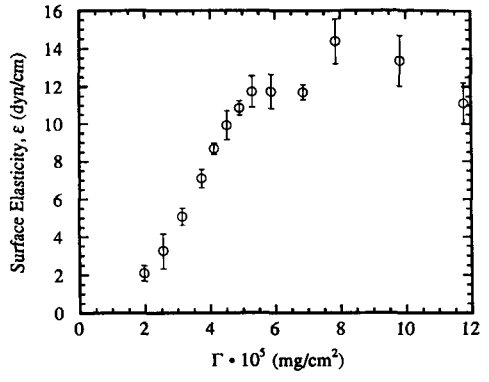

Figure 5 Dynamic surface elasticity as a function of surface concentration for PVAc spread at the air–water interface ($T = 25$°C). The values were computed using data obtained at a frequency of 600 Hz

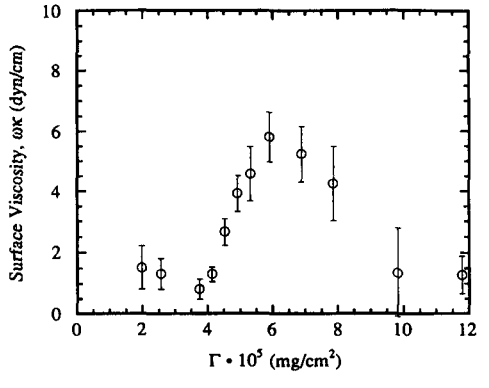

Figure 6 Dynamic surface viscosity (frequency-multiplied) as a function of surface concentration for PVAc spread at the air–water interface ($T = 25$°C). The values were computed using data obtained at a frequency of 600 Hz

waves can easily be observed, especially when the surface layer is covered with a liquid monolayer that supplies more tangential surface stress. As Lucassen-Reynders and Lucassen mentioned in their classic paper[30], the capillary ripples are generally not purely transverse, since there is usually some horizontal surface movement, and the longitudinal wave is not purely longitudinal either, since it involves some vertical surface motion. Usually the appearance of longitudinal waves requires a film coverage of the incompressible subphase since they originate from surface density fluctuation. As a result, the wavelength

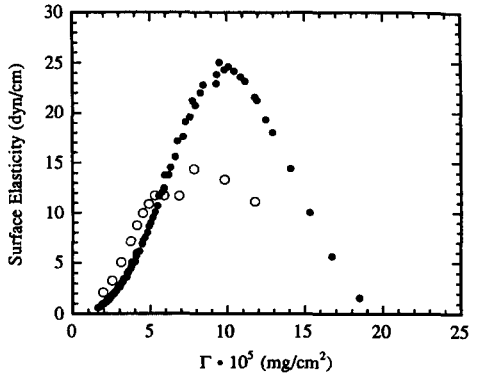

Figure 7 Comparison between static surface elasticity ε_s (●) and dynamic surface elasticity ε (○) obtained from the ECWD measurements ($T = 25$°C), as a function of surface concentration

of the capillary ripple is in general different from that of the longitudinal wave at the same frequency. Hence the horizontal surface deformations are forced to oscillate at frequencies and wavelengths which are not their own. Resonance between the two types of wave motion occurs when the wavelength of the transverse wave at a given frequency is equal to that of the longitudinal wave, and such a resonance results in increased energy losses[30]. Lucassen revealed in his computer calculations[31,32] that the only surface dilational modulus value at which two waves have the same wavelength is the one at the maximum in ripple damping. The maximum observed in the damping constant, $\Gamma = 4.5 \times 10^{-5}$ mg cm^{-2}, represents a resonance behaviour in which the longitudinal waves are coupled to the transverse waves.

As mentioned earlier, by assuming that the transverse viscosity is zero, the complex surface tension is equated to the static surface tension measured for the monolayer[1,3,10]. If we extract surface tension from *Figure 1* at the desired surface concentrations, we can solve the dispersion relation for the surface elasticity, ε, and the surface viscosity, κ. *Figures 5 and 6* are plots of the surface elasticity and the surface viscosity multiplied by the frequency, $\omega\kappa$, as a function of surface concentration. These plots were computed for a frequency of 600 Hz. The surface viscosity and elasticity of PVAc increased significantly at surfactant concentrations between 2×10^{-5} and 6×10^{-5} mg cm^{-2} and between 6×10^{-5} and 8×10^{-5} mg cm^{-2}, respectively. The concentration for maximum damping constant did not coincide with that for maximum surface elasticity or surface viscosity. The maximum damping constant occurs when the wave frequency of the transverse mode is equal to that of the longitudinal mode. This agrees with the experimental results of Vogel and Mobius[26], who found the same surface elasticity and damping constant behaviour for the same PVAc.

Figure 7 compares the dynamic surface elasticity and static surface elasticity, defined as:

$$\varepsilon_s = \Gamma(\partial\pi/\partial\Gamma)_T \qquad (2)$$

The values of ε and ε_s agree relatively well below a concentration of 7×10^{-5} mg cm^{-2}. Above that point, some differences between the ECWD-measured elasticity and the static value are observed. The dynamic surface elasticity measured using SLS and the static value show gratifying agreement over a wide concentration range, as shown in *Figure 8*. It can immediately be imagined that the non-uniformity of PVAc film on the water surface is

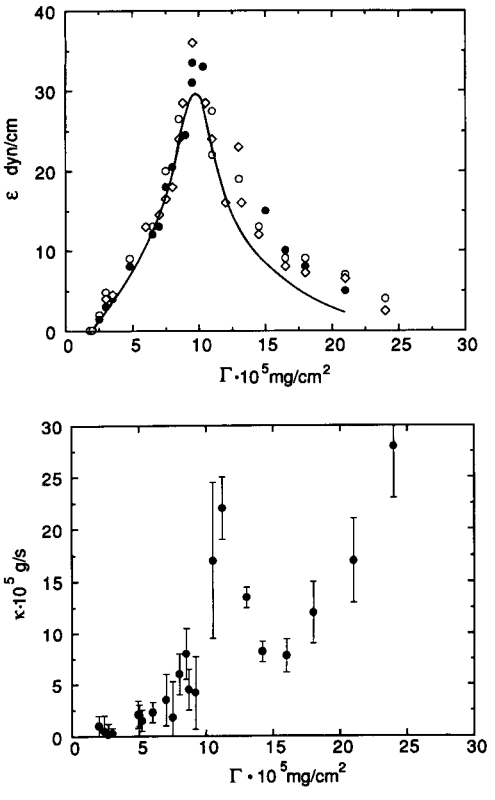

Figure 8 SLS-measured dynamic surface elasticity and viscosity *versus* surface concentration Γ for PVAc. (A) The static dilational elasticity is represented by the solid curve, and the dynamic surface elasticity at different values of k (cm^{-1}): ○, 323; ●, 385; ◇, 445. (B) Dynamic surface viscosity versus Γ for PVAc. The bars represent standard deviations calculated from the variance of the three k values (from ref.15)

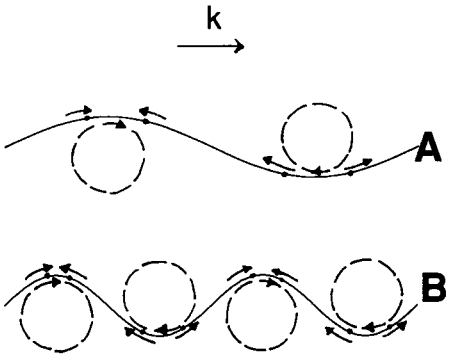

Figure 9 Schematic diagram showing effect of capillary wavelength on surface layer movement. Greater wavelengths can overlook the local compressed and dilated region (A), while small wavelengths can probe details of local movement (B). (Waves are not in real scale ratio: wave in B is exaggerated)

the reason. Non-uniformity refers to the heterogeneous structure of the surface layer. Recently Miyano and Tamada[33,34] investigated capillary wave propagation on water non-uniformly covered with a solid film. According to their experimental results, the equilibrium surface elastic modulus was consistently larger than the dynamic surface elastic modulus.[33] They ascribed this finding to the fact that the film in the liquid phase ('liquid expanded phase') was extremely compressible because the surface waves did not reflect the morphology of the monolayer in the usual capillary wave frequency range. This discrepancy occurs more remarkably when the film is in the solid–gas coexistence phase.[34] The capillary wave propagation characteristics were determined by the connectivity of the solid islands rather than by their coverage. When the film consists of solid islands much smaller than the wavelength, the islands are practically invisible to the wave, even when they cover half the water surface. When the capillary wave trasverses an isolated island much longer than the wavelength, the wave is characterized as one on a solid film of infinite extent. For a surface covered with an inhomogeneous film, the shear stress between the islands should be considered.[35] The compressional (bulk) stress is already transmitted over a long distance when there is a pressure rise and the islands do not affect the capillary wave propagation as long as they can rearrange during one cycle of oscillation.

The tendency of a material to resist the rearrangement of its building blocks under a deformation is the shear rigidity and should manifest itself as a shear stress. However, as shown in *Figure 8*, the agreement in low concentration between the dynamic modulus obtained from the capillary wave experiment and the static modulus calculated from equation (2), which is the bulk modulus only, implies that the shear modulus is negligible. Thus overall surface inhomogeneity does not seem to be the cause of our experimental results. We speculate that the discrepancy is due to the long wavelengths of electrocapillary waves. Since electrocapillary wavelength is much longer than that of thermal capillary waves selected by SLS, it can overlook local density fluctuations which occur because of longitudinal waves (*Figure 9*). As shown in *Figure 8*, the comparison of the static and dynamic surface elasticities by SLS for the same PVAc monolayer on water shows not only that the agreement is quite good, but also that the dynamic value is larger than the static surface longitudinal elasticity, because short wavelengths can probe details of surface particle movement which are in the opposite direction to the wave movement, thus generating a strain that applies a dilational stress to the surface particles[7]. This stress reduces the horizontal motion of the surface particles and increases wave damping. Hence, capillary wave propagation at high frequencies (SLS measurement) would provide better accuracy in probing surface dilational viscoelasticity than that at low frequencies having longer wavelengths (ECWD measurement), as shown in *Figure 9*. This agrees with the observation that there was a clear trend of monotonically decreasing ε with wavelength even though it was not as remarkable in the limited frequency range (<2 kHz). Other experimental results for surface dilational viscoelasticity using ECWD show similar behaviour, i.e. large differences were observed in the high concentration range (in the liquid expanded range)[2,3,19,36]. Another possible reason for the discrepancy is that a relaxation process exists in the low frequency range used in the ECWD study. This possibility would be peculiar to each spread monolayer.[33,37]

The loss tangent, tan δ, is shown in *Figure 10* and is defined as:

$$\tan \delta = (\omega\kappa/\varepsilon) \qquad (3)$$

The viscous contribution to the overall modulus ($\varepsilon^* = \varepsilon + i\omega\kappa$) is equal to the elastic contribution in the low concentration region, but decreases in the high concentration region. Apparently a maximum exists around a concentration of 6×10^{-5} mg cm^{-2}. The peak position where damping is a maximum emerges at a concentration of 6×10^{-5} mg cm^{-2}. Even when we consider inaccuracy at a

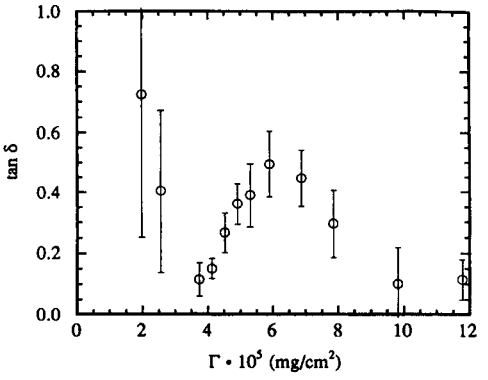

Figure 10 Loss tangent as a function of surface concentration for PVAc spread at the air–water interface ($T = 25°C$). The values were computed using data obtained at a frequency of 600 Hz

high concentration, the value of tan δ shows significant levels of viscoelasticity. Even though the loss modulus term (surface viscosity multiplied by frequency) was of the order of the surface elasticity, pure surface viscosity showed noticeable variation with the frequency, which indicates that a slow intralayer relaxation process would be very important. Since the measurement temperature, 25°C, was close to the glass transition temperature of PVAc, there might have been some relaxation. Because of the relatively narrow frequency range in our experiment (200 Hz–2 kHz), remarkable frequency dependence was not observed. In our surface tension calculation, we neglected the transverse shear viscosity of PVAc, μ, by assuming it to be negligible. However, it may not be zero in a high concentration at 25°C. The effect of increasing μ from zero is to cause ε to decrease and κ to increase[12]. The precise role of transverse viscosity, even though it is negligible in our surface concentration region, should be analysed, especially near the PVAc transition region. Also, it must be remembered that a comparison between ε_s, which was calculated from the π–P isotherm using equation (2) and the dynamic surface elasticity, ε, may not be valid above $\Gamma = 10 \times 10^{-5}$ mg cm^{-2}, since equation (2) is not applicable at the higher concentration where the PVAc segments are presumably leaving the interface[12].

CONCLUSIONS

From the ECWD measurements, the surface elasticity and corresponding viscosity of spread monolayers of PVAc were determined as a function of surface concentration. The maximum damping and maximum surface viscosity occurred at the concentration at which resonance occurred between the transverse and longitudinal capillary waves. The data at the A–W interface were compared with previous results obtained from a capillary wave device operating at high frequencies (SLS). Even though the dynamic surface viscoelastic behaviour was similar in each case, there were some discrepancies between the SLS and ECWD results at a high concentration of PVAc. Similar differences have also been reported by others when ECWD was used. We believe these occurred because of the long capillary wavelength of ECWD, which prevents it from tracing all the movements (surface layer contraction and expansion) of monolayer particles in a highly concentrated region. Hence the dynamic surface elasticity values from ECWD will appear to be smaller than static surface elasticity. On the other hand, dynamic surface elasticity values from SLS can show better agreement with the static surface viscoelasticities because of their short wavelengths in the high concentration region. New information on the role of transverse viscosity is needed for a better understanding of monolayer film properties[12,17,23,24].

REFERENCES

1. Runge, F. E. and Yu, H., *Langmuir*, 1993, **9**, 3191.
2. Gau, C. S., Yu, H. and Zografi, G., *J. Colloid Interface Sci.*, 1994, **162**, 214.
3. Gau, C. S., YU, H. and Zografi, G., *Macromolecules*, 1993, **26**, 2524.
4. Runge, F. E., Kent, M. and Yu, H., *Langmuir*, 1994, **10**, 1962.
5. Earnshaw, J. C. and McCoo, E., *Phys. Rev. Lett.*, 1994, **72**, 84.
6. Lee, K. Y., Chou, T., Chung, D. S. and Mazur, E., *J. Phys. Chem.*, 1993, **97**, 12876.
7. Wang, Q., Feder, A. and Mazur, E., *J. Phys. Chem.*, 1994, **98**, 12720.
8. May, S. E., Gandhi, J. V., Maloy, K. J., Maher, J. V., Kuhar, D. A. and Chapman, T. M., *Macromolecules*, 1993, **26**, 6595.
9. Jiang, Q., Chiew, Y. C. and Valentini, J. E., *Langmuir*, 1992, **8**, 2747.
10. Bonfillon, A. and Langevin, D., *Langmuir*, 1993, **9**, 2172.
11. Bonfillon, A. and Langevin, D., *Langmuir*, 1994, **10**, 2965.
12. Yoo, K. and Yu, H., *Macromolecules*, 1989, **22**, 4019.
13. Sauer, B. B., Kawaguchi, M. and Yu, H., *Macromolecules*, 1987, **20**, 2732.
14. Kawaguchi, M., Sano, M., Chen, Y., Zografi, G. and Yu, H., *Macromolecules*, 1986, **19**, 2606.
15. Kawaguch, M., Sauer, B. B. and Yu, H., *Macromolecules*, 1989, **22**, 1735.
16. Miyano, K., in *Light Scattering by Liquid Surfaces and Complementary Techniques*, Surfactant Science Series Vol. 41, ed. D. Langevin. Dekker, New York, 1992, Ch. 16.
17. Langevin, D., in *Light Scattering by Liquid Surfaces and Complementary Techniques*, Surfactant Science Series Vol. 41, ed. D. Langevin. Dekker, New York, 1992, Chs 7–11.
18. Langevin, D., *Prog. Colloid Polym. Sci.*, 1990, **83**, 10.
19. Ito, K., Sauer, B. B., Skarlupka, R. J., Sano, M. and Yu, H., *Langmuir*, 1990, **6**, 1379.
20. Lucassen-Reynders, E.H. In *Anionic Surfactants*, Surfactant Science Series Vol.11, ed. E. H. Lucassen-Reynders. Dekker, New York, 1981, p. 173.
21. Earnshaw, J. C. and McCoo, E., *Langmuir*, 1995, **11**, 1087.
22. Earnshaw, J. C., McGivern, R. C., McLaughlin, A. C. and Winch, P. J., *Langmuir*, 1990, **6**, 649.
23. Earnshaw, J. C. and McLaughlin, A. C., *Proc. Roy. Soc. Lond. A*, 1993, **A440**, 519.
24. Earnshaw, J. C. and McLaughlin, A. C., *Proc. Roy. Soc. Lond. A*, 1991, **A443**, 663.
25. Earnshaw, J. C., McGivern, R. C. and Winch, P. J., *J. Phys., France*, 1988, **49**, 1271.
26. Vogel, V. and Mobius, D., *Langmuir*, 1989, **5**, 129.
27. De Gennes, P. -G., *Scaling Concepts in Polymer Physics*. Cornell University, Ithaca, NY, 1979.
28. Des Cloizeaux, J., *J. Phys., France*, 1975, **36**, 1199.
29. Kawaguchi, M., Komatsu, S., Matsuzumi, M. and Takahashi, A., *J. Colloid Interface Sci.*, 1984, **102**, 356.
30. Lucassen-Reynders, E. H. and Lucassen, J., *Adv. Colloid Interface Sci.*, 1969, **2**, 347.
31. Lucassen, J., *Trans. Faraday Soc.*, 1968, **64**, 2221.
32. Lucassen, J., *Trans. Faraday Soc.*, 1968, **64**, 2230.
33. Miyano, K. and Tamada, K., *Langmuir*, 1992, **8**, 160.
34. Miyano, K. and Tamada, K., *Langmuir*, 1993, **9**, 508.
35. Chou, T. and Nelson, D. R., *J. Chem. Phys.*, 1994, **101**, 9022.
36. Lemaire, C. and Langevin, D., *Colloids and Surfaces*, 1992, **65**, 101.
37. Mann, E. K. and Langevin, D., *Langmuir*, 1991, **7**, 1112.